


FULL PAPER

Self-organization of micro reinforcements and the rules of crystal formation in polypropylene nucleated by non-selective nucleating agents with dual nucleating ability

Alfréd Menyhárd¹  | János Molnár¹ | Zsuzsanna Horváth² | Flóra Horváth¹ | Dario Cavallo³ | Péter Polyák¹

¹Department of Physical Chemistry and Materials Science, Laboratory of Plastics and Rubber Technology, Budapest University of Technology and Economics, Budapest, Hungary

²Institute of Materials Science and Environmental Chemistry, Research Centre for Natural Sciences, Budapest, Hungary

³Department of Chemistry and Industrial Chemistry, University of Genova, Genova, Italy

Correspondence

Alfréd Menyhárd, Department of Physical Chemistry and Materials Science, Laboratory of Plastics and Rubber Technology, Budapest University of Technology and Economics, H-1111 Budapest Műegyetem rkp. 3. H. ép. I, Hungary.
Email: amenyhard@mail.bme.hu

Funding information

New National Excellence Program of the Ministry for Innovation and Technology, Grant/Award Number: ÚNKP-19-3; Pro Progressio Foundation; Gedeon Richter's Talentum Foundation; Hungarian Academy of Sciences; New National Excellence Program of the Ministry of Human Capacities, Grant/Award Number: ÚNKP-19-4-BME-419

Abstract

This work demonstrates and models the self-organization of mixed polymorphs in polymers containing simultaneously growing phases with different growth rates. The model was verified and demonstrated in isotactic polypropylene nucleated by a non-selective nucleating agent. The crystallization and melting processes were studied by calorimetry (DSC) and polarized light microscopy (PLM). The morphology of the samples was investigated using PLM and scanning electron microscopy (SEM). The fundamental rules of the formation of two polymorphic modifications developing simultaneously on the same nucleating particle are introduced. A simple equation is suggested to predict the morphological geometry on the lateral surface of the nucleating agent. The results indicated good agreement between the predicted and observed geometry. The proposed model explains the self-organization of micro-sized reinforcements of α -modification in the matrix of β -iPP. Although the proposed equation was tested for this particular case it is a general equation for all structures in which different polymorphs are growing simultaneously with different growth rates.

KEYWORDS

dual nucleating ability, mixed polymorphic structure, morphology, nucleating agents, selectivity, self-organization

1 | INTRODUCTION

Nucleating agents (NAs) are used in large amounts to modify the crystalline structure and consequently the properties of semicrystalline polymers.^[1–6] Especially, these additives are used in isotactic polypropylene (iPP), which is the most dynamically developing commercial polymer. The early work of Binsbergen et al.^[1] revealed a few important hints about the correlation between the chemical structure of the NAs and their efficiency, but these correlations were not general. The most probable explanation for nucleation efficiency was given by Alcazar et al.^[7] because they found that the structural matching

between the crystallite sizes results in the nucleating effect. Accordingly, the efficiency of the nucleating agents might be considerably different due to the significantly different morphology of the additives. The reliable comparison of NAs is difficult, but possible using the efficiency scale suggested by Thierry et al.^[8] The effect of these additives is well known, the crystallinity (X) as well as T_{cp} increases in their presence,^[5,9] the crystallization process becomes faster and consequently, the processing of the polymer can be accelerated as well.^[3,5,10] The first NAs applied in large amounts were insoluble in the polymer melt and were dispersed as heterogeneous particles during processing.^[1,11] Consequently, the homogeneous distribution of

This is an open access article under the terms of the Creative Commons Attribution License, which permits use, distribution and reproduction in any medium, provided the original work is properly cited.

© 2020 The Authors. *Polymer Crystallization* published by Wiley Periodicals LLC.

the NA particles is essential, although it is not always easy because of the large aggregation tendency of these additives.^[5] The first breakthrough in this field was the introduction of the sorbitol based NAs by Milliken,^[12–17] which were soluble in the polymer melt at high temperatures and they were designated as organogelators.^[18,19] Nowadays these NAs are used as clarifiers because the nucleus density is very large in their presence.^[15,20–22]

iPP is a polymorphic polymer, which has four crystalline modifications, namely α -, β -, γ -, and the recently discovered ε -forms.^[23–26] Most of the NAs induce the formation of the thermodynamically stable modification of the polymers, thus the majority of NA applied in iPP promote the formation of α -modification.^[3,10,27] There are also numerous NAs, which induce the formation of the β -modification because its impact resistance is significantly larger compared to that of the α -form.^[25,28–39] Several novel β -NAs are soluble in the polymer melt in order to achieve good homogeneity, however, β -NAs are not always completely selective to one of the modifications and mixed polymorphic structure is formed in their presence.^[29,40] This effect is designated as “dual nucleating ability”, which term was introduced in our earlier publication.^[40]

In this work, the crystallization process in the presence of a NA with dual nucleating ability is reported. The rules of the self-organization, as well as the formation of the crystallization process, are described in detail. An equation is suggested, which describes the geometry of the supermolecular structure formed on the surface of nucleating agents with dual nucleating ability. The observations made in this work are easy to implement to any other polymer with complex polymorphic structure.

2 | MATERIALS AND METHODS

Our work focuses on the introduction of the crystallization process on the surface of a non-selective NA in polymorphic polymers. Accordingly, a polymorphic polymer, isotactic polypropylene, was used as model material. Tipplon H890 a commercial grade iPP homopolymer was used in our study to demonstrate that the presented example does not require any special polymer grade. The melt flow rate (MFR) of H890 is 0.3 g/10 minutes (measured at 230°C using 2.16 kg of load).

Two NAs were used in this study. N,N'-Dicyclohexyl-2,6-naphthalenedicarboxamide (NJS),^[41–44] and N,N'-Dicyclohexyl-terephthalamide (DCHT).^[45,46] Their chemical structures are presented in Scheme 1. NJS was added to the iPP in the concentration range of 0 to 1000 ppm, while DCHT was added to the iPP from 0 to 5000 ppm.

The homogenization of the NAs was carried out using a Brabender DSK 4267 twin screw compounder. The temperature profile was 210°C, 220°C, 230°C, 230°C, and the rotating speed was 50 rpm. The extruded fiber was conducted through a water bath, and then it was cut into small granules.

The supermolecular structure of the samples containing NAs was studied by polarized light microscopy (PLM). The measurements were taken using a Zeiss Axioskop equipped by a Leica DMC 320 digital camera and a Mettler FP82 type hot stage. The micrographs were

recorded with the Leica IM50 software. For the determination of the optical character of the samples studied, a λ -plate located diagonally between the crossed polarizers was used. The samples were crystallized under isothermal conditions after the elimination of thermal and mechanical prehistory by heat treatment of the samples at $T_f = 240$ or 250°C for 3 minutes in the presence of NJS or DCHT, respectively. This unusual high T_f was selected in order to study the dissolution of DCHT into the polymer melt. After the heat treatment, the samples were cooled to various crystallization temperatures (T_c) at a rate of $5^\circ\text{C}/\text{min}$ or quenched at $20^\circ\text{C}/\text{min}$ to T_c .

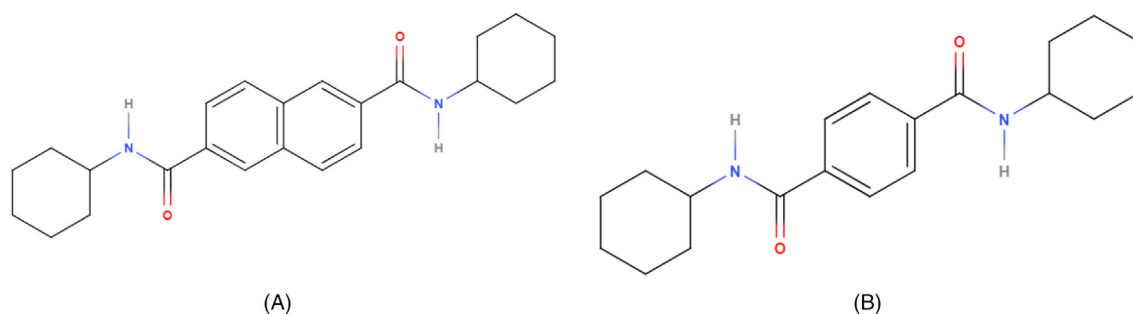
SEM micrographs were taken from the samples using JEOL ISM 5600 LV equipment. The surface of the samples was etched with a permanganate solution^[47] for 24 hours at room temperature in order to observe the fine morphology in details.

3 | CRYSTALLIZATION MODEL

Here we introduce a simple approach, which describes the geometrical rules of the crystallization process of the polymorphic modifications on the surface of the NA with dual nucleating ability.

In an earlier publication we discussed a soluble β -NA which was proved to have dual nucleating ability in iPP.^[40] To demonstrate the way it affects the crystalline structure of the polymer we present a schematic illustration of the initial (a) and the later (b) stages of the crystallization process in Figure 1. In this particular case the α - and the β -modifications developed simultaneously on the surface of the NA crystals.

Although the polymorphic forms can develop simultaneously on the surface of the NA crystal, the nucleation density of the different forms is usually also different because of the dissimilar efficiency of the NA for each modification. The nucleation density of a polymorphic modification on the surface of the NA crystal is proportional to the efficiency of the NA to that certain form. As a consequence, the type of the NA (and thus the nucleation density) together with the growth rates of the modifications will determine the final crystalline structure. Essentially, despite the simultaneous formation of the nuclei of the different polymorphic forms during crystallization only that modification will develop in which more nuclei are induced and has a growth rate (G) higher or at least equal to that of the other forms. In our case below 100°C ($T_{\alpha\beta}$) and above 140°C ($T_{\beta\alpha}$) only the thermodynamically stable α -iPP develops, because it has a higher growth rate than the β -iPP.^[48,49] If the conditions of crystallization favor the growth of the β -form (ie, the temperature is between $T_{\alpha\beta}$ and $T_{\beta\alpha}$), the formation of this less stable modification is also feasible as it is presented in Figure 1. Fan-like formations of the β -modification develop in the early stage of the crystallization. The slower modification will be overgrown by these fan-like structures and small occluded crystals will remain near the surface of the NA. The ratio of the growth rates (R) determines the shape and the size of these small occluded crystals as well as the center angle of the fan-like formations. By varying the temperature of crystallization the structure can be tuned.



SCHEME 1 Chemical structure of A, NJS and B, DCHT

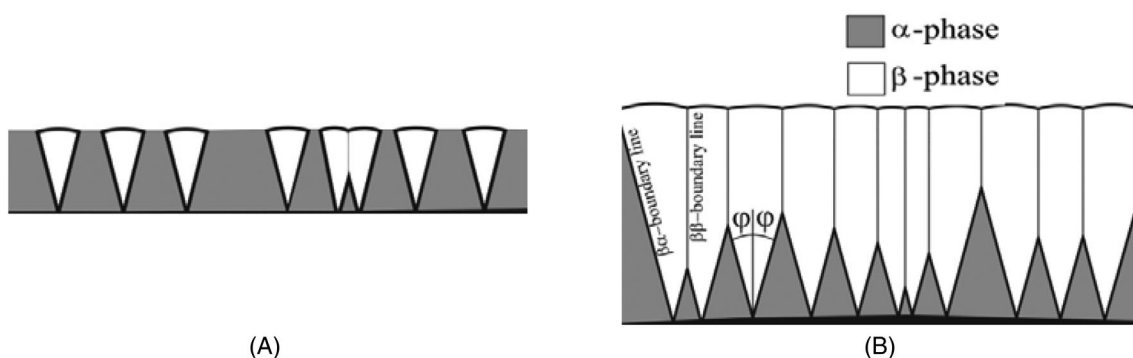


FIGURE 1 Simultaneous crystallization of the α - and β -modifications of iPP on the surface of a NA with dual nucleating ability in A, the initial and B, the later stages of the crystallization process if the temperature is between $T_{\alpha\beta}$ and $T_{\beta\alpha}$. NA, nucleating agent

$$R = \frac{G_{\text{faster}}}{G_{\text{slower}}} = \frac{G_{\beta}}{G_{\alpha}} \quad (1)$$

In Equation (1) R is calculated by dividing the higher growth rate with the lower one, thus R always has a value larger than 1. In our case, if the temperature is between $T_{\alpha\beta}$ and $T_{\beta\alpha}$, the growth rate of the β -form has to be divided by that of the α -modification as it is demonstrated in Equation (1). We have to note that the growth rates depend on temperature thus the calculation of R may change accordingly in other cases. The precise geometrical calculation of the shape of the fan-like slices is possible in analytical geometry similarly to the earlier work by Varga^[50], but first, the following preconditions should be considered.

- The α -nuclei form in large density at $t = 0$ minute along the entire planar surface of the nucleating agent (x -axis)
- The sole β -nucleus (which can form sporadically) is located exactly in the origin and starts growing also at $t = 0$ minute

A lack of the β -nucleus in the origin would eventuate a formation of α -crystals along the entire x -axis, which would grow at a constant rate independent from the x spatial coordinate. The interface (y) between the melt and the already crystalline phase would be, therefore, a straight line parallel with the x -axis:

$$y = G_{\alpha} \cdot t \quad (2)$$

Where G_{α} refers to the growth rate of α -modification, t is the denomination of the time coordinate. The case we are intending to investigate now, however, features a sole β -nucleus located in the origin (see the above introduced initial conditions). Unlike the α -form nucleated along the entire x -axis, β -phase starts to grow from a single point ($x = 0$, $y = 0$, that is, the origin), which eventuates the formation of a circular spherulite of a radius (r_{β}) determined solely by the time coordinate:

$$x^2 + y^2 = r_{\beta}(t)^2 = [G_{\beta} \cdot t]^2 \quad (3)$$

The interface between the α - and β -phases are determined by the points being capable of simultaneously satisfy Equations (2) and (3), which point is reached by both α - and β -forms at the same time (Equation (4)). By changing the time, these points will give the borderline between the α - and β -crystals.

$$G_{\alpha} \cdot t = y \quad \text{and} \quad G_{\beta} \cdot t = y \quad (4)$$

In simpler words: the interface between the adjacent α - and β -phases is lying along a set of points marked by (x , y) coordinates reached by the continuously growing α - and β -phase at the exact same time. This means, that Equations (2) and (3) needs to be solved simultaneously. A solution requires one equation to be eliminated first, for example, by expressing the variable of time from Equation (2):

$$\frac{1}{G_\alpha} \cdot y = t \quad (5)$$

Which can now be substituted back into Equation (3):

$$x^2 + y^2 = \left[\frac{G_\beta}{G_\alpha} \cdot y \right]^2 \quad (6)$$

As the brackets on the right side contain a simple product, the y coordinate can be separated from the parameters of the growing rates:

$$x^2 + y^2 = \left(\frac{G_\beta}{G_\alpha} \right)^2 \cdot y^2 \quad (7)$$

After the rearrangement of Equation (7), the following equation can be written:

$$x^2 = \left(\frac{G_\beta}{G_\alpha} \right)^2 \cdot y^2 - y^2 \quad (8)$$

Equation (8) can be re-written and rearranged as:

$$x^2 = \left[\left(\frac{G_\beta}{G_\alpha} \right)^2 - 1 \right] \cdot y^2 \quad (9)$$

$$\frac{x^2}{y^2} = \left(\frac{G_\beta}{G_\alpha} \right)^2 - 1 \quad (10)$$

Note that both of the variables located on the left side are squared, their ratio, therefore, can be simplified:

$$\left(\frac{x}{y} \right)^2 = \left(\frac{G_\beta}{G_\alpha} \right)^2 - 1 \quad (11)$$

A ratio of the spatial coordinates can now be expressed as a square root of the right side of Equation (11):

$$\frac{x}{y} = \sqrt{\left(\frac{G_\beta}{G_\alpha} \right)^2 - 1} \quad (12)$$

At this point, one might consider, that x and y coordinates are projections of the end of the hypotenuse (outlined by the interface between the α - and β -phases) to the abscissa and ordinate, respectively. Therefore, the angle we are searching for can be expressed by using these coordinates: as x equals to the opposite cathetus, while y equals to the adjacent cathetus, their ratio—by definition—is expected to be equal to the tangent of the angle confined by the y -axis and the interface line between the alpha and beta phase.

$$\tan(\varphi(G_\alpha, G_\beta)) = \frac{x}{y} = \pm \sqrt{\left(\frac{G_\beta}{G_\alpha} \right)^2 - 1} \quad (13)$$

In order to express the angle itself, one might apply the inverse function of a tangent:

$$\varphi(G_\alpha, G_\beta) = \arctan \left[\pm \sqrt{\left(\frac{G_\beta}{G_\alpha} \right)^2 - 1} \right] \quad (14)$$

Introducing Equation (1) into Equation (14) the central φ angle can be obtained as:

$$\varphi(G_\alpha, G_\beta) = \arctan \left[\pm \sqrt{R^2 - 1} \right] \quad (15)$$

Figure 2A demonstrates the correlation between the φ angle and R in the case of iPP (the growth rates of α - and β -modifications were taken from earlier works^[48]) and Figure 2B is the graphical representation of Equation (15). It should be noted that as the growth rate is somewhat dependent on the molecular structure of the polymer the data given in Varga's work may not apply for all iPP grades. Nonetheless, the ratio of the growth rates is less sensitive to the molecular structure than the primary G data of the modifications, thus the data presented by Varga for iPP can be used for prediction.

4 | RESULTS AND DISCUSSION

Figure 2A illustrates that the φ angle increases monotonously with increasing R which implies that the fan-like structures are wider if the difference of the growth rates increases. This theory was corroborated by experimental results. In Figure 3 the microscopic view of the crystallization process on the surface of a needle like NA with dual nucleating ability is presented. The sample was nucleated by 500 ppm NJS and was heated to 240°C before crystallization so that the NJS dissolves completely. The NA was recrystallized in needle form at 190°C and subsequently, the sample was cooled to the crystallization temperature of 135°C. We show in Figure 3 the structure of the crystalline phase developed on the lateral surface of the NJS needle. The value of R at 135°C was taken from the work of Varga et al.^[48] and it equals to 1.178. The φ angle was calculated using this value according to Equation (15), and the result is 22.2°. Compared this calculated angle to the measured value (22.0 ± 2.65° Figure 3B) it can be established that the experimental and simulated values are in excellent agreement despite the fact that different iPP grades were used in the two studies. Accordingly, the good agreement supports our assumption that R is less sensitive to the polymer grade than the primary G data. We have to note that the measurements of the central angle from PLM figure is complicated thus the values obtained from microscopic pictures have a certain scattering.

It should be noted, that the growth rate of α -iPP becomes faster above $T_{\beta\alpha}$ and consequently a modification change takes place above this temperature on the surface of the β -crystals. This interesting phenomenon is called "cross-nucleation" and it has anomalous temperature dependence as it was described recently.^[51,52] Our general

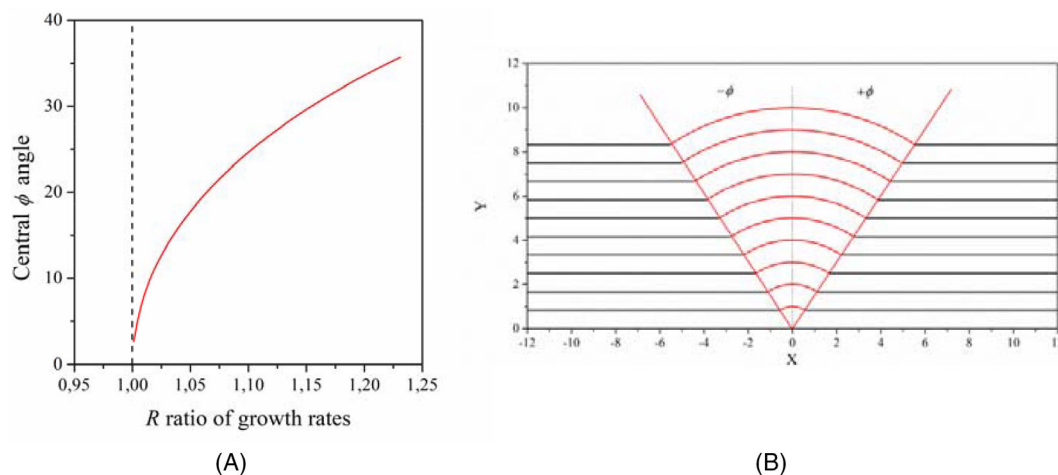


FIGURE 2 Simulated ϕ angle according to Equation (15) as a function of the ratio between the growth rates of A, β - and α -iPP and B, a schematic representation of the structure. All data presented in this figure are based on the growth rate data measured by Varga et al.^[48]

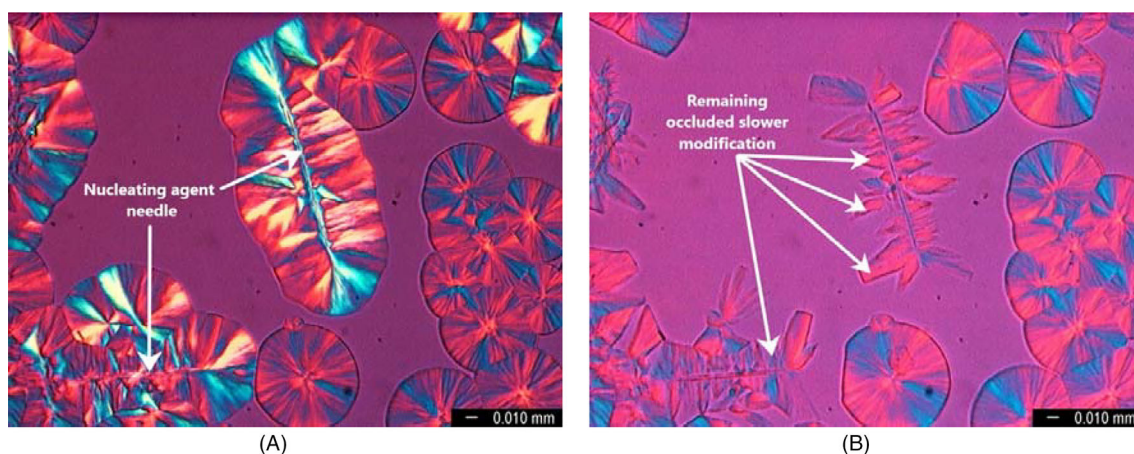


FIGURE 3 Crystallization representing similar structure than Figure 2 in practice in the presence of NJS at A, 135°C for 30 minutes and after the partial melting of β -iPP at B, 156°C

model can be applied for the description of this phenomenon as well because it is also the development of different modifications on a surface, but the surface is the growing β -spherulite.

5 | MODELL APPLICATION: CROSS-NUCLEATION

In this particular case (above $T_{\beta\alpha}$) R should be defined as G_{α}/G_{β} , because at this temperature the α -modification grows faster. The ratio of R can be estimated from the review work of Varga, where the cross-nucleation phenomenon was described in detail.^[53] The process is presented in Figure 4.

The cross nucleation was studied in this review work at 141.5°C (above $T_{\beta\alpha} = 140^{\circ}\text{C}$), where R is close to 1 (actually $R = 1.075$) and the cross nucleation density is very low. At this temperature, the growth rate of α -modification is a little faster than that of the β -form. Based

on the detailed study of reverse temperature dependency of cross nucleation,^[51] its rate is slow and in this case, the study of individual cross nuclei is possible. The structure presented in Figure 4 was prepared during a two-step crystallization process. The sample was crystallized at 135°C for a long time where large spherulites (β -iPP at the left-hand side and α -iPP at the right-hand side) were developed. Subsequently, crystallization temperature was raised to 141.5°C, where slow cross nucleation occurred. After the cross nucleated slices became clearly observable, the temperature was elevated further to 163.5°C, where β -modification melted completely. Consequently, the α -form developed during cross nucleation became well observable. The predicted angle is 21.5° and the measured values are $21.5 \pm 3.5^{\circ}$. We have to note here that cross nucleation takes place at the curved surface of a growing spherulite, but Equation (15) can be used for calculating the ϕ angle even in this case as well. However, the boundaries of the faster spherulite slice will be a Limaçon curve instead of a straight line. The derivation of this case is presented in the Supporting

Information as well. As it was pointed out in our earlier work, “cross-nucleation” has reverse temperature dependency, thus the number of the cross nuclei increases with temperature.^[51] Apparently, φ angle may be larger than the predicted far above $T_{\beta\alpha}$, because several nuclei may form very close to each other and those cannot be distinguished and studied individually.

The detailed explanation of the crystallization process in the presence of additives with dual nucleating ability allows us to understand the crystallization process under real industrial conditions. According to our model, if the crystallization takes place in the temperature range between $T_{\alpha\beta}$ and $T_{\beta\alpha}$, which range overlaps mostly with the temperature range of crystallization during conventional processing technologies, fan-like β -slices should overgrow the slower α -iPP (See in Figure 3). The structure demonstrated in Figure 3, however, cannot be obtained under real industrial processing parameters, because the crystallization runs under dynamic cooling conditions. If the cooling rate is higher, the NA cannot develop needle crystals, so it recrystallizes in the form of smaller and finely dispersed crystals instead. Still,

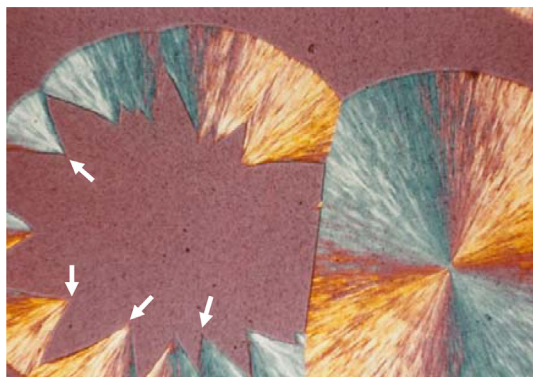


FIGURE 4 The cross nucleation process on the surface of a β -iPP spherulite after raising the temperature above the critical $\beta\alpha$ -recrystallization temperature at 141.5°C. The φ angles were measured at the locations marked by arrows

the rules of crystallization proposed above are valid also in the case of these smaller crystals. To demonstrate this process a sample containing NJS in a very small amount (50 ppm) was quenched to the crystallization temperature in PLM. The sample was heated to 240°C to dissolve the entire amount of NA and then it was cooled to the crystallization temperature. In this case, the recrystallization and self-organization of the nucleating agent as well as the crystallization of the polymer occur simultaneously. This process is rather similar to the industrial conditions, however under processing conditions the cooling rate is even higher and the nucleating agent content is also larger (Figure 5). At the center of the micrograph a “microcrystalline” structure developed, which consists of the small α -crystals overgrown by the β -iPP matrix. Here the nucleating agent recrystallized locally during crystallization, because its concentration increases in the free melt phase where large spherulites were not formed. Although the crystals of the nucleating agent are not observable, after the partial melting of the β -phase at 156°C the small α -crystals can be visualized. At a larger NA content this structure becomes homogeneous, but the phenomena can be demonstrated more clearly using this small concentration.

At larger NA content (2000 ppm DCHT) the structure is more homogeneous and the self-organized microcrystalline structure covers almost all the view area of the microscope (see in Figure 6). The crystallization was conducted at 135°C, in order to keep T_c between $T_{\alpha\beta}$ and $T_{\beta\alpha}$. It is well discernable that well-developed spherulites cannot form because of the large nucleating agent content. For better visualization of the overgrown α -crystals, the λ -plate was removed from the microscope and the structure was captured in black and white color. The self-organization of the finely distributed α -crystals is similar to the expected structure under real processing conditions, however, the size of the small inclusions could be even smaller in that case.

In order to check the structure formed under real industrial conditions, NJS was added to the iPP in 500 ppm and standard ISO 527 specimens were injection molded under conventional conditions. The temperature of the melt was 240°C and the mold temperature was

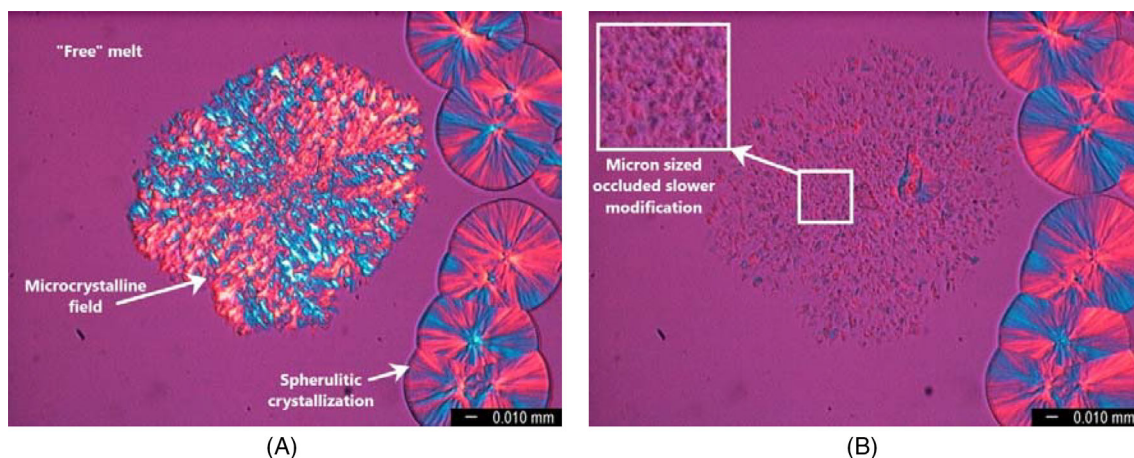


FIGURE 5 “Microcrystalline” field formed in the presence of 50 ppm NJS at A, 135°C and the remaining small α -crystals after the partial melting of β -iPP at B, 156°C

FIGURE 6 Crystalline structure formed in the presence of 2000 ppm DCHT at A, 135°C and the residual small α -crystals after the partial melting of β -iPP at B, 156°C. The sample was heated to 250°C in order to dissolve the NA and then was cooled directly to the crystallization temperature as fast as possible. NA, nucleating agent

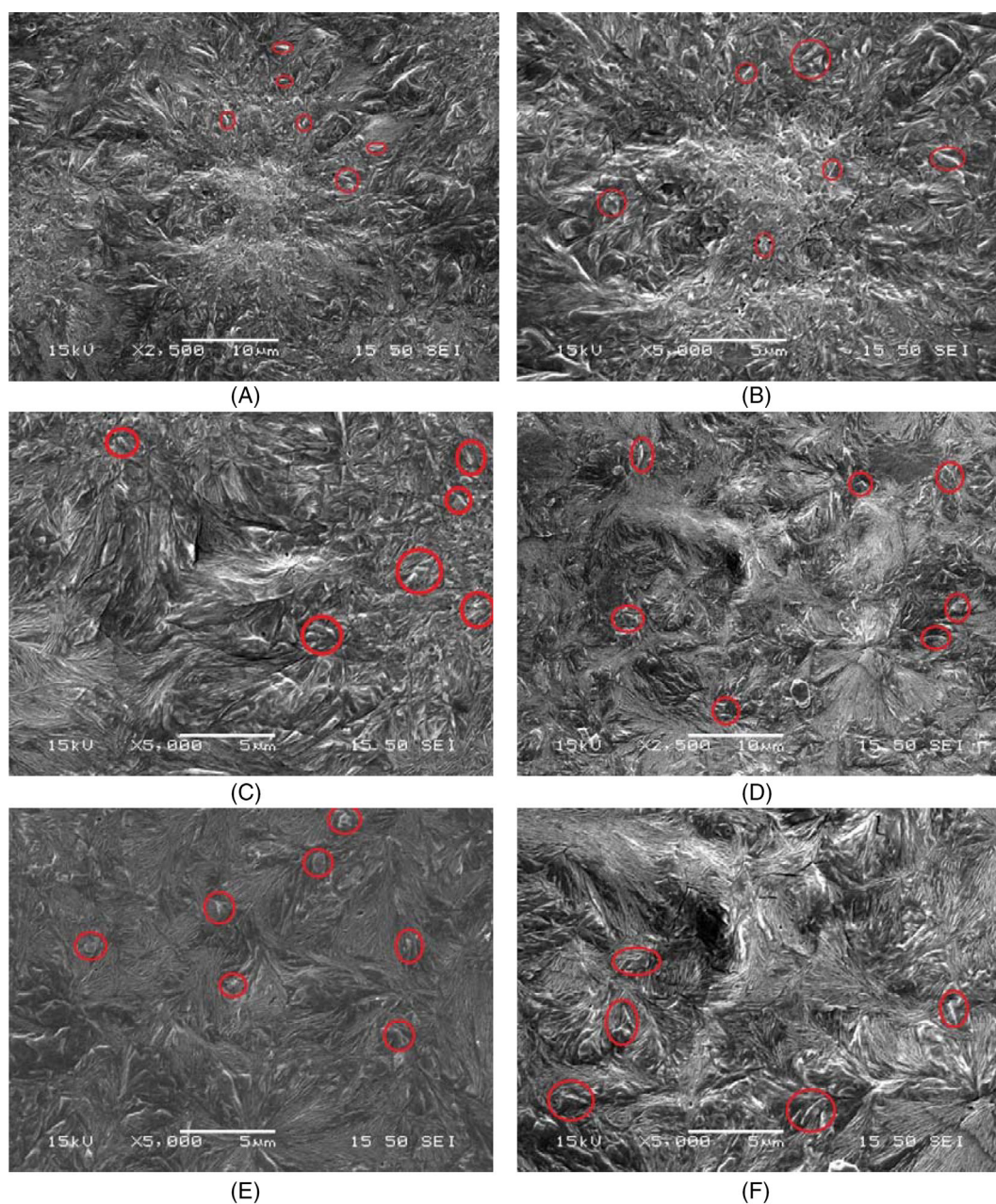
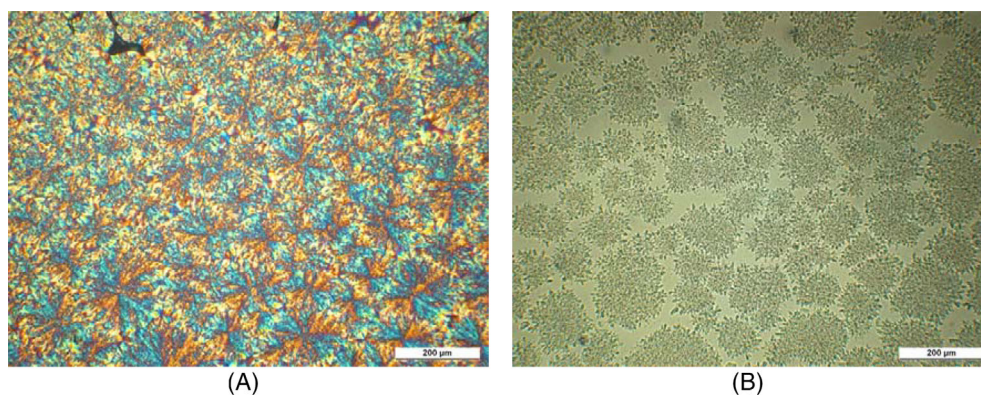


FIGURE 7 Crystalline structure observed on the fracture surface of the specimens fabricated for mechanical tests. A,B,C, NJS 500 ppm and D,E,F, 300 ppm NJS in different magnifications and locations. The samples were fractured in liquid nitrogen in order to avoid plastic deformation. Then the fracture surface was etched for 48 hours using a permanganic etching solution according to Olley and Bassett^[47]

40°C, thus the cooling rate is certainly faster in the injection molding process than 20°C/min, thus all the required conditions were fulfilled. The supermolecular structure formed during the real processing conditions was studied on the fracture surfaces (Figure 7), which were etched using etching solution according to Olley et al.^[47]

It is known that α -iPP dissolves even slower during etching, thus the sharp small crystals represent the reinforcing α -crystals (few of them are marked in Figure 7), which can be observed in large density in these samples. The final structure is formed throughout the recrystallization and self-organization of the nucleating agent and then the dual crystallization process of the polymer. Consequently, the amount of reinforcing α -crystals can be manipulated by the content of the NA because more and more NA particles form as a consequence of the recrystallization of the NA and proportionally the amount of the small micron-sized α -crystals increases as well. This is the explanation for the fact that the partial fraction of α -modification increases slightly with increasing of nucleating agent content.^[29,40,45] The model and the self-organized structure presented here explains clearly that small α -crystals reinforces the β -iPP matrix in injection molded specimens resulting in simultaneous stiffening and toughening effect, which was observed by us and other researchers as well.^[45,54–56]

6 | CONCLUSIONS

The crystallization process was discussed in this work in the presence of soluble nucleating agents with dual nucleating ability. The general rule of crystallization on the surface of a non-selective nucleating agent was explained in detail and using a simple geometrical model. The reliability of the proposed model was proved in the case of the crystallization on the surface of a non-selective β -nucleating agent and in the case of “cross nucleation” as well. The agreement between the predicted and the measured angles is good in both cases indicating the model is generally valid and robust. It was proved clearly that a special self-organizing structure develops in iPP the presence of nucleating agents with dual nucleating ability, in which small α -crystals are distributed finely in a β -matrix. It was proved that this structure develops under conventional processing conditions as well and this structure can explain clearly the advantageous mechanical properties of iPP in the presence of nucleating agent with dual nucleating ability. We have to state that the proposed model is not limited to iPP and it could be adapted to any other polymorphic polymer, in which nucleating agents with dual nucleating ability are used.

ACKNOWLEDGMENTS

The first Author of this work (Alfréd Menyhárd) would like to express his indebtedness to his former professor (József Varga) and dedicate this paper to him. Prof. Varga has passed away in 2015, but he has started this research and revealed the dual nucleating activity of the non-selective nucleating agents in the iPP. His inspiring atmosphere was the cradle of this work. This work was supported by the ÚNKP-19-4-BME-419 New National Excellence

Program of the Ministry of Human Capacities and by the János Bolyai Scholarship of the Hungarian Academy of Sciences. One of the authors (Flóra Horváth) would like to express her gratitude to Gedeon Richter's Talentum Foundation (1103 Budapest, Gyömrői út 19-21.) and to Pro Progressio Foundation for their financial support. This work was also supported by the ÚNKP-19-3 New National Excellence Program of the Ministry for Innovation and Technology.

CONFLICT OF INTEREST

The authors declare no potential conflict of interest.

AUTHOR CONTRIBUTIONS

Alfréd Menyhárd is the corresponding Author. He contributed in the preparation of the microscopic studies, building the main geometrical approach and he prepared the final version of the manuscript. János Molnár, Zsuzsanna Horváth and Flóra Horváth contributed to the experimental work. Especially they did the electron microscopic studies. Dario Cavallo provided the cross nucleation data and Péter Polyák did the mathematical derivations mostly.

ORCID

Alfréd Menyhárd  <https://orcid.org/0000-0002-7133-0918>

REFERENCES

- [1] F. L. Binsbergen, *Polymer* **1970**, *11*, 253. [https://doi.org/10.1016/0032-3861\(70\)90036-4](https://doi.org/10.1016/0032-3861(70)90036-4).
- [2] K. Mitsubishi, Polypropylene, Nucleating Agents. in *The Polymeric Materials Encyclopedia*, Vol. 9, (Ed: J. C. Salamone), CRC Press, Boca Raton, FL, USA **1996**, p. 6602.
- [3] S. Fairgrieve, *Rapra Rev. Rep.* **2005**, *16*, 1.
- [4] D. Libster, A. Aserin, N. Garti, *Polym. Adv. Technol.* **2007**, *18*, 685. <https://doi.org/10.1002/pat.970>.
- [5] M. Gahleitner, C. Grein, S. Kheirandish, J. Wolfschwenger, *Int. Polym. Proc.* **2011**, *26*, 2. <https://doi.org/10.3139/217.2411>.
- [6] H. N. Beck, *J. Appl. Polym. Sci.* **1967**, *11*, 673. <https://doi.org/10.1002/app.1967.070110505>.
- [7] D. Alcazar, J. Ruan, A. Thierry, B. Lotz, *Macromolecules* **2006**, *39*, 2832. <https://doi.org/10.1021/ma052651r>.
- [8] A. Thierry, B. Fillon, C. Straupé, B. Lotz, J. Wittmann, *Progr. Colloid Polym. Sci.* **1992**, *87*, 28. <https://doi.org/10.1007/BFb0115569>.
- [9] J. Menczel, J. Varga, *Journal of Thermal Analysis* **1983**, *28*, 161. <https://doi.org/10.1007/BF02105288>.
- [10] E. P. Moore, *Polypropylene Handbook: Polymerization, Characterization, Properties, Processing, Applications*, Hanser-Gardner Publications, Cincinnati **1996**, p. 1.
- [11] F. L. Binsbergen, *J. Polym. Sci. Polym. Phys. Ed.* **1973**, *11*, 117. <https://doi.org/10.1002/pol.1973.180110112>.
- [12] T. L. Smith, D. Masilamani, L. K. Bui, R. Brambilla, Y. P. Khanna, K. A. Gabriel, *J. Appl. Polym. Sci.* **1994**, *52*, 591. <https://doi.org/10.1002/app.1994.070520502>.
- [13] K. Bernland, J. G. P. Goossens, P. Smith, T. A. Tervoort, *J. Polym. Sci. Pt. B Polym. Phys.* **2016**, *54*, 865. <https://doi.org/10.1002/polb.23992>.
- [14] K. Bernland, T. Tervoort, P. Smith, *Polymer* **2009**, *50*, 2460. <https://doi.org/10.1016/j.polymer.2009.03.010>.
- [15] P. M. Kristiansen, A. Gress, P. Smith, D. Hanft, H. W. Schmidt, *Polymer* **2006**, *47*, 249. <https://doi.org/10.1016/j.polymer.2005.08.053>.

- [16] M. Kristiansen, M. Werner, T. Tervoort, P. Smith, M. Blomenhofer, H. W. Schmidt, *Macromolecules* **2003**, 36, 5150. <https://doi.org/10.1021/ma030146t>.
- [17] M. Kristiansen, T. Tervoort, P. Smith, *Polymer* **2003**, 44, 5885. [https://doi.org/10.1016/S0032-3861\(03\)00538-X](https://doi.org/10.1016/S0032-3861(03)00538-X).
- [18] A. Thierry, C. Straupe, J. C. Wittmann, B. Lotz, *Macromol. Symp.* **2006**, 241, 103. <https://doi.org/10.1002/masy.200650915>.
- [19] Z. Horváth, B. Gyarmati, A. Menyhárd, P. Doshev, M. Gahleitner, J. Varga, B. Pukánszky, *RSC Adv.* **2014**, 4, 19737. <https://doi.org/10.1039/c4ra01917b>.
- [20] A. Menyhárd, M. Bredács, G. Simon, Z. Horváth, *Macromolecules* **2015**, 48, 2561. <https://doi.org/10.1021/acs.macromol.5b00275>.
- [21] F. Santis, R. Pantani, *J. Therm. Anal. Calorim.* **2013**, 112, 1481. <https://doi.org/10.1007/s10973-012-2732-5>.
- [22] A. Menyhárd, M. Gahleitner, J. Varga, K. Bernreitner, P. Jääskeläinen, H. Řyscđ, B. Pukánszky, *Eur. Polym. J.* **2009**, 45, 3138. <https://doi.org/10.1016/j.eurpolymj.2009.08.006>.
- [23] F. J. Padden, H. D. Keith, *J. Appl. Phys.* **1959**, 30, 1479. <https://doi.org/10.1063/1.1734985>.
- [24] S. Brückner, S. V. Meille, V. Petraccone, B. Pirozzi, *Prog. Polym. Sci.* **1991**, 16, 361.
- [25] J. Varga, *J. Macromol. Sci. Part B-Phys.* **2002**, 41(4-6), 1121. <https://doi.org/10.1081/MB-120013089>.
- [26] B. Lotz, *Macromolecules* **2014**, 47, 7612. <https://doi.org/10.1021/ma5009868>.
- [27] J. Varga, Crystallization, Melting and Supramolecular Structure of Isotactic Polypropylene. in *Polypropylene: Structure, Blends and Composites*, Vol. 1, (Ed: J. Karger-Kocsis), Chapman&Hall, London **1995**, p. 56.
- [28] C. Mathieu, A. Thierry, J. C. Wittmann, B. Lotz, *J. Polym. Sci. Pt. B-Polym. Phys.* **2002**, 40, 2504.
- [29] A. Menyhárd, J. Varga, G. Molnár, *J. Therm. Anal. Calorim.* **2006**, 83, 625. <https://doi.org/10.1007/s10973-005-7498-6>.
- [30] Q. Dou, Q. L. Lu, H. D. Li, *J. Macromol. Sci. Part B Phys.* **2008**, 47, 900.
- [31] S. Zhao, Z. Cai, Z. Xin, *Polymer* **2008**, 49, 2745. <https://doi.org/10.1016/j.polymer.2008.04.012>.
- [32] Q. Dou, *J. Appl. Polym. Sci.* **2009**, 111, 1738.
- [33] Z. S. Zhang, C. Y. Chen, C. G. Wang, Z. A. Junping, K. C. A. Mai, *Polym. Int.* **2010**, 59, 1199. <https://doi.org/10.1002/pi.2847>.
- [34] A. R. Zeng, Y. Y. Zheng, S. C. Qiu, Y. Guo, *J. Appl. Polym. Sci.* **2011**, 121, 3651.
- [35] D. G. Papageorgiou, G. Z. Papageorgiou, D. N. Bikiaris, K. Chrissafis, *Eur. Polym. J.* **2013**, 49, 1577. <https://doi.org/10.1016/j.eurpolymj.2013.02.002>.
- [36] J. S. Hu, J. Sun, D. Su, X. J. Yao, *Int. J. Polym. Anal. Charact.* **2014**, 19, 661. <https://doi.org/10.1080/1023666x.2014.953764>.
- [37] Y. J. Li, M. E. Li, M. Nie, Q. Wang, R. Han, *J. Mater. Sci.* **2017**, 52, 981. <https://doi.org/10.1007/s10853-016-0393-7>.
- [38] Q. Sheng, Y. Zhang, C. Xia, D. Mi, X. Xu, T. Wang, J. Zhang, *Mater. Des.* **2016**, 95, 247. <https://doi.org/10.1016/j.matdes.2016.01.114>.
- [39] Y. F. Zhang, H. H. Hou, L. H. Guo, *J. Therm. Anal. Calorim.* **2018**, 131, 1483. <https://doi.org/10.1007/s10973-017-6669-6>.
- [40] J. Varga, A. Menyhárd, *Macromolecules* **2007**, 40, 2422. <https://doi.org/10.1021/ma062815j>.
- [41] Ikeda, N.; Kobayashi, T.; Killough, L. In *Novel Beta-Nucleator for Polypropylene*, Polypropylene '96. World Congress, Zürich, Switzerland, Sept. 18–20., 1996; Zürich, Switzerland, **1996**.
- [42] Y. Q. Shi, Z. Xin, *J. Thermoplast. Compos. Mater.* **2016**, 29, 1667. <https://doi.org/10.1177/0892705715583178>.
- [43] K.-J. Zhan, W. Yang, L. Yue, B.-H. Xie, M.-B. Yang, *J. Macromol. Sci. Part B Phys.* **2012**, 51, 2412. <https://doi.org/10.1080/00222348.2012.676366>.
- [44] M. Yamaguchi, T. Fukui, K. Okamoto, S. Sasaki, Y. Uchiyama, C. Ueoka, *Polymer* **2009**, 50, 1497.
- [45] F. Horváth, T. Gombár, J. Varga, A. Menyhárd, *J. Therm. Anal. Calorim.* **2017**, 128, 925. <https://doi.org/10.1007/s10973-016-6057-7>.
- [46] Y. Xu, H. Du, M. Gu, *Petrochem. Technol.* **2013**, 42, 1148.
- [47] R. H. Olley, D. C. Bassett, *Polymer* **1982**, 23, 1707. [https://doi.org/10.1016/0032-3861\(82\)90110-0](https://doi.org/10.1016/0032-3861(82)90110-0).
- [48] J. Varga, Y. Fujiwara, A. Ille, *Period. Polytech. Chem. Eng.* **1990**, 34, 255.
- [49] B. Monasse, J. M. Haudin, *Colloid Polym. Sci.* **1985**, 263, 822. <https://doi.org/10.1007/BF01412960>.
- [50] J. Varga, *Die Angew. Makromol. Chem.* **1983**, 112, 161. <https://doi.org/10.1002/apmc.1983.051120111>.
- [51] S. Looijmans, A. Menyhard, G. W. M. Peters, G. C. Alfonso, D. Cavallo, *Cryst. Growth Des.* **2017**, 17, 4936. <https://doi.org/10.1021/acs.cgd.7b00872>.
- [52] S. F. S. P. Looijmans, D. Cavallo, L. Yu, G. W. M. Peters, *Cryst. Growth Des.* **2018**, 18, 3921. <https://doi.org/10.1021/acs.cgd.8b00254>.
- [53] J. Varga, *J. Mater. Sci.* **1992**, 27, 2557. <https://doi.org/10.1007/BF00540671>.
- [54] F. Horváth, J. Molnár, A. Menyhárd, Polypropylene Nucleation. in *Polypropylene Handbook: Morphology, Blends and Composites*, (Eds: J. Karger-Kocsis, T. Bárány), Springer International Publishing: Cham, Switzerland **2019**, p. 121.
- [55] Y. Uchiyama, S. Iwasaki, C. Ueoka, T. Fukui, K. Okamoto, M. Yamaguchi, *J Polym Sci B* **2009**, 47, 424.
- [56] R. Yang, L. Ding, X. Zhang, J. C. Li, *Ind. Eng. Chem. Res.* **2018**, 57, 2083. <https://doi.org/10.1021/acs.iecr.7b04115>.

SUPPORTING INFORMATION

Additional supporting information may be found online in the Supporting Information section at the end of this article.

How to cite this article: Menyhárd A, Molnár J, Horváth Z, Horváth F, Cavallo D, Polyák P. Self-organization of micro reinforcements and the rules of crystal formation in polypropylene nucleated by non-selective nucleating agents with dual nucleating ability. *Polymer Crystallization*. 2020; e10136. <https://doi.org/10.1002/pcr2.10136>